DISCIPLINARUM SCIENTIA *Disciplinarum Scientia.* **Série: Naturais e Tecnológicas**
Santa Maria, v. 26, n. 2, p. 51-64, 2025
Recebido em: 24.11.2024. Aprovado em: 04.04.2025.
ISSN 2176-462X | DOI: doi.org/10.37779/nt.v26i2.5182

ADSORPTION OF THE RHODAMINE B DYE USING RICE HUSK ASH[1]

ADSORÇÃO DO CORANTE RODAMINA B USANDO CINZAS DE CASCA DE ARROZ

Fabiane Figueiredo Severo[2], Pâmela Cristine Ladwig Muraro[3], Jivago Schumacher de Oliveira[4], Luiz Fernando Rodrigues Junior[5], William Leonardo da Silva[6] e Maria Amélia Zazycki[7]

ABSTRACT

Synthetic dyes have been used in various industrial processes, mainly in the textile, food, paper and paint sectors. It is of great environmental importance that the effluents generated in these industries are treated before being released into water resources. Adsorption is one of the most used methods in the treatment of water contaminated by dyes due to its high efficiency and low operating cost. Thus, the study investigated the potential use of rice husk ash for the removal of rhodamine B (RhB) dye in aqueous solution. Rice husk ash was obtained from the process of burning rice husk, without temperature and exposure time control and denominate CA1 and CA2. The ash was characterized regarding physical and chemical characteristics. The adsorption capacity was 2.59 and 3.25 mg g-1 for the ashes tested with a percentage of dye removal of 32.13% and 36.06% for CA1 and CA2, respectively. The adsorption kinetics of RhB on both ashes followed the pseudo-first order model. Equilibrium isotherms were well represented for the Langmuir and Freundlich model. In summary, it was possible to add value to rice ash residues, generating a low-cost adsorbent to treat colored effluents.

Keywords: Waste; Environmental impact; Ecosystems.

RESUMO

Corantes sintéticos têm sido utilizados em diversos processos industriais, principalmente nos setores têxtil, alimentício, de papel e tintas. É de grande importância ambiental que os efluentes gerados nessas indústrias sejam tratados antes de serem lançados em recursos hídricos. A adsorção é um dos métodos mais utilizados no tratamento de águas contaminadas por corantes devido à sua alta eficiência e baixo custo operacional. Assim, o estudo investigou o potencial uso de cinzas de casca de arroz para a remoção do corante rodamina B (RhB) em solução aquosa. As cinzas de casca de arroz foram obtidas a partir do processo de queima da casca de arroz, sem controle de temperatura e tempo de exposição e denominadas CA1 e CA2. As cinzas foram caracterizadas quanto às características físicas e químicas. A capacidade de adsorção foi de

1 Trabalho final de graduação em Engenharia Ambiental e Sanitária.

2 Autora. Engenheira Ambiental. E-mail: fabifsr.qmc@gmail.com. ORCID: https://orcid.org/0000-0003-2821-5882

3 Coautora. Pós doutoranda UTEC. E-mail: pamelamuraro@ufn.edu.br. ORCID: https://orcid.org/0000-0002-8791-7633

4 Coautor. Professor do Programa de Pós-graduação em nanociências. E-mail: jivago@ufn.edu.br. ORCID: https://orcid.org/0000-0003-2772-0801

5 Coautor. Professor do Programa de Pós-graduação em Saúde Materno Infantil. E-mail: luiz.fernando@ufn.edu.br. ORCID: https://orcid.org/0000-0002-5753-5503

6 Coautor. Professor do Programa de Pós-graduação em nanociências. E-mail: w.silva@ufn.edu.br. ORCID: https://orcid.org/0000-0002-7804-9678

7 Orientadora. Professora do Curso de Engenharia Química. E-mail: zazycki@ufn.edu.br. ORCID: https://orcid.org/0009-0008-8638-3124

2,59 e 3,25 mg g-1 para as cinzas testadas com uma porcentagem de remoção de corante de 32,13% e 36,06% para CA1 e CA2, respectivamente. A cinética de adsorção de RhB em ambas as cinzas seguiu o modelo de pseudo-primeira ordem. As isotermas de equilíbrio foram bem representadas para o modelo de Langmuir e Freundlich. Em resumo, foi possível agregar valor aos resíduos de cinza de arroz, gerando um adsorvente de baixo custo para tratar efluentes coloridos.

Palavras-chave: *Resíduos; Impacto ambiental; Ecossistemas.*

INTRODUCTION

According to the World Health Organization (Who, 2019), approximately 13 million people die annually due to poor environmental conditions, such as lack of access to clean water for basic needs. It was possible to affirm that one of the main causes of water pollution was the increase in industrial activities in recent decades (Alcântara, 2016). Industries related to the most different activities collaborate with this pollution, but those in the textile sector are considered as the largest generators of water waste, it is known that about 150 liters of water are needed to produce one kilo of fabric, and of this volume, 88% are discarded as liquid effluents and 12% are lost by evaporation (Grassi *et al.*, 2012). The effluent generated by these industries has dyes and these, in turn, can be detected with the naked eye due to the presence of color. The presence of dyes in wastewater alters the ecosystem, as it prevents the incidence of sunlight radiation in the aquatic environment, affecting the metabolism of plants and animals (Kant, 2012; Boer, 2013).

Rhodamine B (RhB) is a cationic and hydrophilic synthetic dye, which has been widely used in the textile, leather, paper and printing industries. This dye has a fluorescent property and is therefore also used as a molecular probe (Gong *et al.*, 2016) and electrochemical luminescence sensor (Li *et al.*, 2012). In addition, it is used as a pathological marker in laboratory tests (Cheng and Tsai, 2016). Its presence in wastewater released to the environment has caused great environmental concern, due to the resistance that this dye has to degrade naturally. RhB has chemical stability and a complex molecular structure, becoming a recalcitrant dye that is difficult to remove (Machado *et al.*, 2012). About human health, its toxicity was related to irritations in the eyes, airways and, it has carcinogenicity and neurotoxicity (Rodrigues, 2015).

The removal of these dyes from wastewater is a major environmental challenge for these industries and there is a constant need to have an effective process for this purpose. In this context, the literature shows a series of treatment technologies (Katheresan *et al.*, 2018), being that, adsorption stands out due its efficiency, in terms of low cost, ease of implementation and operation, and high efficiency of removal of toxic contaminants (Zazycki *et al.*, 2018). Currently, the material widely used to remove colors from effluents is activated carbon, but its high cost limits the application of this method (Gautam *et al.*, 2014). Thus, research has been developed as alternative materials that have good adsorption capacity and lower cost (Oliveira *et al.*, 2018), such as nanozeolite doped with silver

and titanium nanoparticles (Oviedo *et al*., 2022), magnetic graphene oxide (Vargas *et al*., 2023) and magnetic carbon nanotubes derivatives (Salles *et al*., 2023).

The use of agro-industrial residues, such as pyrolyzed rice husk in the form of ash, can be an alternative to reduce RhB dye in the industrial effluents using the adsorption process. The state of Rio Grande of Sul is the largest rice producer in Brazil (Severo, 2019) and using rice husk would not be a technical and operational limitation. In addition, rice husks are a material of difficult decomposition in the environment and are widely used in heat generation in drying ovens of grains and thermoelectric plants. For example, each tonne (ton) of rice produces about 200 kg of husk, which, by combustion, generates around 40 kg of ash, constituting a raw material of low cost and high availability (Cortez *et al*., 2008).

Thus, the study investigated the potential use of rice husk ash for the removal of the RhB dye in aqueous solution. Rice husk ash was obtained from different burning conditions and were characterized, regarding its function groups, crystallinity, and textural properties. Last, the adsorbents employed RhB adsorption kinetics and equilibrium. In this way, the novelty of the study is to promote added value to an agroindustrial waste for the treatment of dye-containing wastewater meeting the theme of sustainable development with the Sustainable Development Goals (SDGs).

MATERIAL AND METHODS

MATERIALS ACQUISITION

Both rice husk ashes (CA1) and (CA2) were collected from two different local rice trade companies Primo Berleze & Cia and processing of J. Fighera & Cia rice in Santa Maria, RS, respectively. The rice husk ash was obtained from the furnaces employed on the heat generation, without firing control. The CA1 had a longer exposure in the furnace in comparison with the CA2. After that, the ashes were disposed of on the ground in open air, and collections were randomly carried out in piles, being packed in plastic bags for transportation and subsequent analysis. There was no pretreatment or drying done on material.

The dye used was Rhodamine RhB (Vetec, PA) and 100 mL of solution at a concentration of 1 g L^{-1} was used for the adsorption tests. The chemical structure of the dye is shown in Figure 1.

Figure 1 - Chemical structure of RhB.

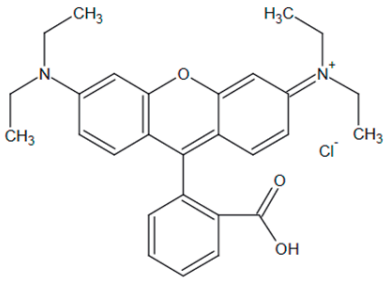

Chemical Formula: $C_{28}H_{31}ClN_2O_3$

Molecular Weight: 479 g mol^{-1}

CAS number: 81-88-9

Source: Authors.

CHEMICAL AND PHYSICAL CHARACTERIZATION OF RICE ASH

Total carbon (C) and nitrogen (N) contents of ashes were determined using elemental Analyzer (Flash model EA-1112, Thermo Scientifics). For elemental composition, 200 mg of each material were burnt in a muffle at 500 °C for 8 hrs and digestion was carried out with a mixture of nitric acid and hydrogen peroxide (Enders *et al*., 2012). The calcium (Ca), magnesium (Mg), iron (Fe), manganese (Mn), copper (Cu) and zinc (Zn) content were measured by atomic absorption spectrometer (AAnalyst 200 - PerkinElmer), except for phosphorus (P) by using spectrophotometer (BEL Model S05) (Murph and Riley, 1962).

The cation exchange capacity (CEC) was determined according to Silva (2009) and the neutralization power (NP) was determined by the same procedure used for lime described by Brasil (2014); however, the solutions used had to be diluted in relation to the original methodology, given the low neutralization power of the materials. Surface acid groups (carboxylic acids, phenols and lactones) were estimated by return titration as described in Boehm (1994). Determination of the ash content made according to ASTM D3172-13 (ASTM, 2013). The specific surface area (SSA) was determined by the BET procedure in an automatic determiner (Quantachrome Instruments) at the Ceramic Materials Laboratory (LACER) of the Federal University of Rio Grande do Sul (UFRGS).

The ashes samples were characterized by X-ray diffraction (X-ray diffraction DXA, Advance Bruker), after milling in mortar and pistil, sieved in 45-micron mesh and powdered in the equipment. The analyzes were performed at room temperature with a copper tube (Kα = 1.5418 Å radiation), in a range of 2θ of 10º-70º, with resolution of 0.02º and 0.6 s count time. The samples were also grind in mortar and pistil, mixed with potassium bromide (KBr), pressed and characterized by Fourier Transform Infrared Spectroscopy (FTIR) in spectrophotometer (Spectro One model, Perkin-Elmer) to identify functional groups at the Department of Material Engineering of the Franciscan University (UFN).

Malvern-Zetasizer equipment® NanoZS model with closed hair cells (DTS 1060) was used to measure the zeta potential values of the target molecule and biosorbent (peel), serving as a parameter for the determination of the pH point of zero charge (pHpzc), where 50 mg of the respective rice

husks were put in contact with 50 mL of adsorbate aqueous solution (RhB), under different initial pH (2.3; 4.3; 6.4; 7.8, 10.3 and 11.7) and the charge surface was measured after 24 hours of contact. All measurements were performed in triplicates.

ADSORPTION TESTS

The adsorption tests were carried out in a batch regime, according to the literature (Oliveira, 2013). Initially, 100 mL of RhB aqueous solution (60 mg L^{-1}) were placed in contact with 100 mg of dry ash under magnetic agitation (150 rpm) for 120 minutes. During agitation, samples of 1 mL were collected and stored in Eppendorfs® at predetermined times (0, 5, 15, 30, 45, 60, 75, 90, and 120 minutes), to verify the variation of RhB dye concentration with time at room temperature (25ºC ± 2ºC). Finally, this concentration variation was determined in a spectrophotometer (Cary 100 Scan, UV-Vis Spectrophotometers, United States) at the characteristic wavelength of RhB (553 nm). The experiments were carried out in triplicate and blanks were performed. The dye removal percentage (R, %), adsorption capacity at any time t (qt, mg g^{-1}) and the equilibrium adsorption capacity (qe, mg g^{-1}), were determined by Equations 1, 2 e 3, respectively:

$$R = \frac{(C_0 - C_f)}{C_0} \quad (1)$$

$$q_t = \frac{V(C_0 - C_t)}{m} \quad (2)$$

$$q_e = \frac{V(C_0 - C_e)}{m} \quad (3)$$

Where, C0 is the initial dye concentration in the liquid phase (mg L^{-1}), Cf is the final dye concentration in the liquid phase (mg L^{-1}), Ct is the dye concentration in liquid phase at any time (mg L^{-1}), Ce is the dye concentration in the liquid phase at equilibrium (mg L^{-1}), V is the solution volume (L), m is the adsorbent mass (g).

KINETIC AND EQUILIBRIUM ADSORPTION

The kinetic models involving the RhB dye adsorption with CA's were studied using the pseudo first-order (PFO)and pseudo second-order (PSO) models, according to the Equations 4 and 5, respectively (Qiu *et al.*, 2009).

$$q_t = q_1.(1 - exp\ exp\ (-k_1.t)) \quad (4)$$

$$q_t = \frac{t}{\left(\frac{1}{k_2.q_2^2}\right)+\left(\frac{t}{q_2}\right)} \quad (5)$$

Where: k_1 (min^{-1}) rate constant of pseudo first-order; q_1 (mg g^{-1}) theoretical value of adsorption capacity; k_2 (g mg−1 min−1) rate constant of pseudo-second order; q_2 (mg g^{-1}) theoretical value of adsorption capacity.

The adsorption equilibrium isotherms were adjusted using the Langmuir (Equation 6) (Langmuir, 1918) and Freundlich (Equation 7) (Freundlich, 1906) models.

$$q = \frac{q_m \cdot K_L \cdot C_{eq}}{1 + K_L \cdot C_{eq}} \quad (6)$$

$$q = K_F \cdot C_{eq}^{\frac{1}{n}} \quad (7)$$

Where: q_m (mg g^{-1}) maximum adsorption capacity; k_L (L mg^{-1}) Langmuir constant; k_F (mg g^{-1}) (mg L^{-1}) $^{-1/n}$ Freundlich constant; 1/n heterogeneity factor.

Moreover, an essential characteristic of Langmuir isotherm was represented by the separation factor or equilibrium parameter (R_L), which indicates the shape of the isotherm and the nature of the adsorption process whether it was favorable or not, was determined by Equation 8.

$$R_L = \frac{1}{1 + K_L.C_0} \quad (8)$$

Where: $R_L > 1$: unfavorable adsorption; R_L: linear; $0 < R_L < 1$: favorable adsorption; $R_L = 0$: irreversible process.

STATISTICAL ANALYSIS

The kinetic and equilibrium parameters were determined by adjusting the models with the experimental data, using nonlinear regression. Statistica 10 software (StatSoft, USA) was used to perform the calculations, applying the Quasi-Newton estimation method.

RESULTS AND DISCUSSION

CHEMICAL AND PHYSICAL CHARACTERIZATION OF RICE ASH

The CA2 presented higher C content compared to CA1 (Table 1). Virtually, no N was detected in ashes. Higher Si content was verified in both ashes. There was no significant difference in Mn, Mg,

Ca, Cu, Fe, K, and P contents among ashes, which are in relatively low concentrations, except for P and K, which presented higher values compared to the others. The ashes presented low neutralization power (NP), although different from each other (Table 1). A higher CEC value was obtained in the CA2 compared to CA1. The presence of carboxylic radicals (-COOH) was not detected. The phenolic groups (-OH) were higher in relation to the lactonic groups (-COOR).

According to table 1, the specific surface area (SSA) of rice husk ash (CA1 and CA2) was measured as 9.2 $m^2 g^{-1}$ for CA1 and 9.5 $m^2 g^{-1}$ for CA2, values considered relatively low compared to other adsorbent materials, such as carbons developed from pecan nutshells, chitin, and MDF residues, which exhibit surface areas of 93 $m^2 g^{-1}$, 275 $m^2 g^{-1}$, and 218.8 $m^2 g^{-1}$, respectively (Zazycki *et al.*, 2018, 2019, 2020). This low surface area can be attributed to the prolonged exposure to heat without controlled burning, which likely reduced porosity and caused particle sintering, as well as the absence of chemical treatments, which could have increased the surface area and reactivity of the material. The predominant composition of amorphous silica (SiO_2) in the ash also contributes to the limited surface area, as silica in its natural form tends to be less porous.

Table 1 - Chemical and physical parameters of ashes CA1 and CA2.

Chemical and physical parameters	CA1 (mean value ± SD)	CA2 (mean value ± SD)
Carbon (%)	0.93 ± 0.05 c	16.5 ± 2.11 b
Nitrogen (%)	<0.01b	0.01 b
Oxygen (%)	26.5 ± 2.1 a	14.5 ± 1.7 c
Silicon (%)	66.0 ± 8.5 a	59.5 ± 7.8 b
Manganese (g kg^{-1})	0.32 ± 0.04	0.45 ± 0.11
Magnesium (g kg^{-1})	1.09 ± 0.43	0.69 ± 0.08
Calcium (g kg^{-1})	1.28 ± 0.53	1.00 ± 0.01
Cooper (g kg^{-1})	0.03 ± 0.02	0.01
Zinc (g kg^{-1})	0.13 ± 0.01 b	0.12 ± 0.01 b
Iron (g kg^{-1})	0.37 ± 0.10	0.34 ± 0.04
Potassium (g kg^{-1})	6.2 ± 1.81	5.3 ± 0.37
Phosphorus (g kg^{-1})	3.1 ± 0.70	2.5 ± 1.29
Ash (%)	96.0 ± 0.15 b	68.9 ± 1.44 c
Neutralizing power (%)	0.51 ± 0.02 b	0.44 ± 0.04 c
Carboxylic groups ($mmol_c$ g^{-1})	<0.01	<0.01
Lactonic groups ($mmol_c$ g^{-1})	4.5 ± 0.2 a	2.7 ± 0.2 c
Phenolic groups ($mmol_c$ g^{-1})	6.2 ± 0.2 c	9.5 ± 0.2 b
CEC* (cmolc kg^{-1})	40.0 ± 5 c	57.5 ± 2.5 b
SSA** (m^2 g^{-1})	9.2 ± 0.24 c	9.5 ± 1.18 bc

*Cation Exchance Capacity **Specific Surface Area. Means followed by distinct letters in horizontal line have significant differences according to the Tukey's test ($p<0.05$).
Source: Authors.

The Fourier transform infrared (FTIR) absorption spectra of the adsorbents are shown in Figure 2, where bands characteristic of the stretching modes of the O-Si bond in polymorphic silicas

(SiO_2) (Chaves *et al*., 2009) at 1100 cm^{-1} and 800 cm^{-1}. The band at 1100 cm^{-1} is attributed to the asymmetric vibrational stretching of the SiO_4 tetrahedron, while that at 800 cm^{-1} indicates the O-H bond of the silanol groups (Akhtar *et al*., 2010). Moreover, the transmittance peak between 3678 and 3272 cm^{-1} present in ashes indicates the presence of hydroxyl groups (-OH). These groups may be derived from phenols, alcohols, ethers, and esters. The band in 1617 cm^{-1} shows the stretch related to aldehydes.

Figure 2 - FTIR spectra of the CA1 and CA2.

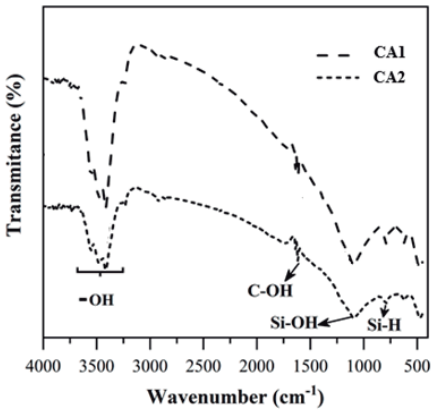

Source: Authors.

The ashes of rice hulls showed silicate structures in crystalline arrangements in the XRD evaluation (Figure 3). In CA1 It was possible to verify the occurrence of silicate phases (quartz and cristobalite) verified, as well as the presence of Ca in its crystalline structure (gyrolineite). The CA2 presented phases with the presence of silica (cristobalite) and K.

Figure 3 - X-ray diffraction of ashes CA1 (A) and CA2 (B) of rice husks.

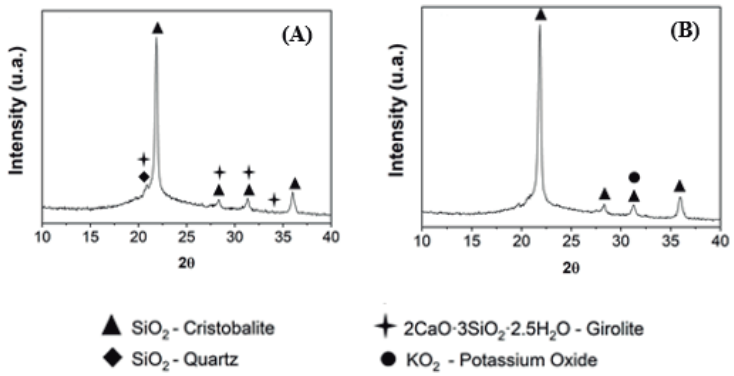

Source: Authors.

According to Figure 4, the pH_{pzc} was determined at the intersection point of the curve, where the pH_{pzc} becomes constant, being equal to 11.5 for both adsorbents. Moreover, when the pH of the medium was lower than the pH_{pzc}, the adsorbent material was positively charged (protonated), favoring the adsorption of compounds with negative charges, and a large number of anions are adsorbed to balance positive charges, such as anionic dyes. When the pH of the medium was greater than the $pH_{pzc,}$

the adsorbent was negatively charged (deprotonated), favoring the adsorption of compounds with positive net loads (Castilla, 2004). Moreover, RhB dye solution showed pH ≈ 4.3, while the surface charge of adsorbents was positive (protonated) (pH < pH_{ZCP}), favoring the adsorption of negative species, confirmed by cation exchange capacity (CTC) (40 and 57 comic kg^{-1} CA1 and CA2, respectively) and that 100% of CA1 and 85% of CA2 were occupied by Fe^{2+} adsorption (Severo *et al.*, 2020).

Figure 4 - Zeta potential according to the pH solution for the CA1 and CA2.

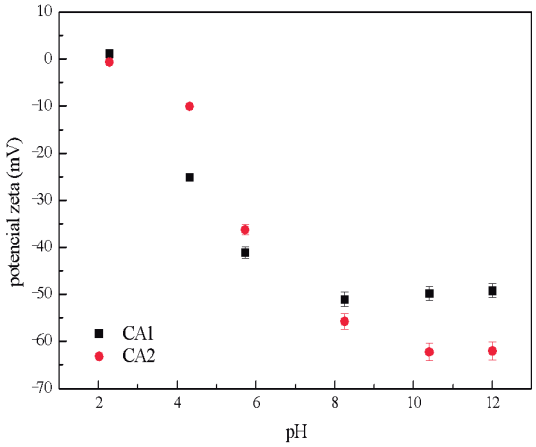

Source: Authors.

KINETIC STUDY

Figure 5 (a) and (b) showed the kinetic study using CA1 and are CA2, respectively. Moreover, Table 2 showed the kinetic parameters obtained for the PPO and PSO models.

Figure 5- Kinetic curves for RhB adsorption in (a) CA1 and (b) CA2 (T = 298 K; adsorbent concentration = 1.0 g L^{-1}; dye concentration= 60 mg L^{-1} and pH ≈ 4.3).

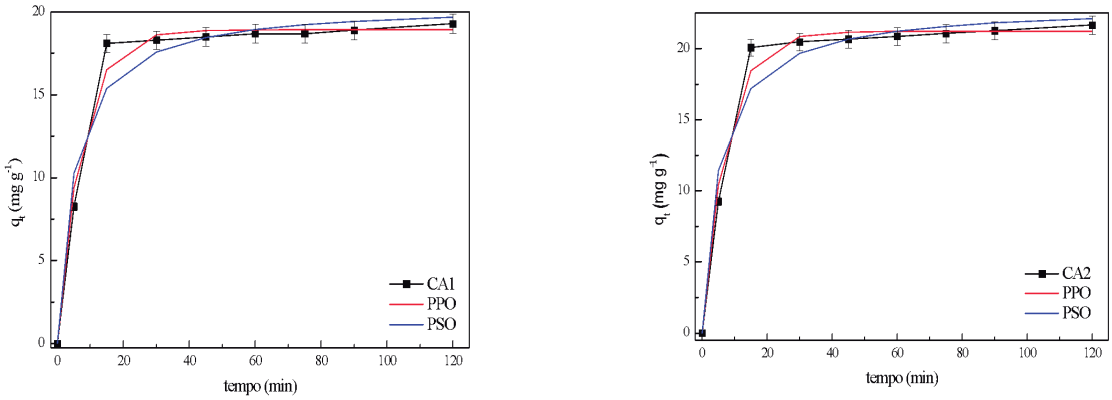

(a) (b)

Source: Authors.

Table 2 - Kinetic parameters for RhB adsorption in CA1 and CA2.

Kinetic model	**Adsorbent**	
Pseudo-first-order	**CA1**	**CA2**
q_1 (mg g^{-1})	18.92 ± 0.05	21.20 ± 0.05
k_1 (min^{-1})	0.14 ± 0.05	0.13 ± 0.05
R^2	0.988	0.989
Pseudo-second-order	**CCA1**	**CCA2**
q_2 (mg g^{-1})	20.51 ± 0.05	23.01 ± 0.05
k_2 (g mg^{-1} min)	0.01 ± 0.05	0.09 ± 0.05
R^2	0.965	0.968

Source: Authors.

As shown in Figure 5**,** typical kinetic curves were obtained, where a rapid initial step of up to 10 min was observed for both ashes. For all initial dye concentrations, equilibrium was reached within 40 min. The maximum adsorption capacity was 20.51 and 23.01 mg L^{-1} for CA1 and CA2, respectively. This is interesting for wastewater treatment plants, considering that a high amount of dye is removed from the liquid in short time intervals. According to Table 2, the parameters of linear regressions determined using kinetic models, which reveal the pseudo-first-order equation, provided the best adjustments of the experimental data, indicating primarily the external diffusion as the controlling step, and independent of the concentration of adsorbate, prevailing mass transfer between adsorbent and RhB (Malik, 2003).

EQUILIBRIUM STUDY

Table 3 shows the results obtained from the adjustments to the Langmuir and Freundlich isotherm models, based on the experimental data.

Table 3 - Equilibrium parameters for RhB dye adsorption with CA1 and CA2.

Isotherm model	**Biosorbent**		
	Parameter	**CA1**	**CA2**
Langmuir	Qmax (mg g^{-1})	2.59 ± 0.05	3.25 ± 0.05
	L_R	0.17 ± 0.05	0.35 ± 0.05
	R^2	0.994	0.990
Freundlich	n	3.62 ± 0.05	3.11 ± 0.05
	R^2	0.998	0.997

Source: Authors.

According to Table 3, the maximum adsorption capacity found was 2.59 and 3.25 mg g^{-1} for the adsorbents CA1 and CA2, respectively. In addition, both materials present favorable adsorption, represented by the equilibrium parameter (K_L) between 0 and 1, as removal of 32.13% (CA1) and 36.06% (CA2), after 120 minutes. About the equilibrium parameters of the Freundlich model,

it was possible to identify a favorable adsorption process for both adsorbent materials, since $1< n < 10$ (Nascimento *et al.*, 2014). On the experimental data, the results adjust for both models (Langmuir and Freundlich) indicating complete monolayer adsorption for non-uniform sites, characteristic of heterogeneous systems (Gupta *et al.*, 2009).

The lower removal efficiency of rice husk ash (CA1 and CA2) compared to other adsorbents reported in the literature (Table 4) can be explained by several factors. The prolonged exposure to heat without controlled burning likely reduced the porosity and surface area of the ash, limiting its adsorption capacity. Additionally, the ash was not subjected to chemical treatments, which could have increased its surface area and reactivity. The nature of the Rhodamine B dye, with its large and complex molecular structure, may also have hindered adsorption, especially at relatively high concentrations (60 mg L^{-1}). In contrast, many other adsorbents, such as bamboo and Pinus sawdust, exhibit greater porosity, surface area, and, in some cases, undergo chemical treatments that enhance their efficiency, resulting in higher removal rates (73.7% to 94.6%). Given these results, it is necessary to investigate whether the activation of the ash could improve its removal efficiency. However, this process may compromise the feasibility of using the ash on an industrial scale due to increased costs and operational complexity. Therefore, to improve the performance of rice husk ash, it would be necessary to optimize burning conditions, functionalize the surface, or test the material at lower dye concentrations, seeking a balance between efficiency and technical feasibility.

Table 4 - Alternative adsorbents in the removal of dyes in aqueous solutions.

Adsorbent	Adsorbate	Adsorbate (mg L^{-1})	% removal	Reference
Bamboo charred sawdust	Methylene blue	200	93,1	Kannan (2001)
Dalbergia sissoo (sawdust treated with sulfuric acid)	Methylene blue	250	82,2	Garget (2004)
Dalbergia sissoo (sawdust treated with formaldehyde)	Methylene blue	250	73,7	Garget (2004)
Wood sawdust	*Direct green 26*	500	78,8	Antunes *et al.* (2010)
Dust sawdust Pinus *sp.*	Methylene blue	150	81,8	Ikeno (2013)
Dust sawdust Pinus *sp.*	Malachite green	9	94,6	Silva (2014)

Source: Authors.

CONCLUSION

This study demonstrates the potential of rice husk ash (RHA), an abundant agro-industrial waste, as a low-cost and sustainable adsorbent for Rhodamine B (RhB) dye removal from aqueous solutions. The characterization of RHA samples (CA1 and CA2) revealed a predominance of amorphous silica with low specific surface areas (9.2-9.5 m^2 g^{-1}), attributed to uncontrolled combustion conditions and inherent material limitations. Despite these constraints, the adsorption experiments achieved removal efficiencies of 32.13% (CA1) and 36.06% (CA2), with equilibrium capacities of 2.59 and 3.25 mg g^{-1}, respectively. Kinetic analysis indicated that the adsorption process followed a

pseudo-first-order model, suggesting surface diffusion as the dominant mechanism. Equilibrium data were well-described by both Langmuir and Freundlich isotherms, implying monolayer adsorption on heterogeneous surfaces.

While RHA's performance is inferior to activated carbon or chemically modified adsorbents, its advantages lie in its low cost, minimal processing requirements, and alignment with circular economy principles. The use of RHA not only addresses dye pollution but also valorizes agricultural waste, reducing environmental burdens associated with disposal. To enhance adsorption efficiency, future studies should explore optimized combustion parameters, surface functionalization, or hybrid treatments to improve porosity and reactivity.

This work highlights the feasibility of integrating agro-industrial residues into wastewater treatment strategies, contributing to Sustainable Development Goals (SDGs) 6 (Clean Water and Sanitation) and 12 (Responsible Consumption and Production). Further research should focus on scaling up the process and evaluating economic viability for industrial applications, ensuring a balance between efficiency, sustainability, and practicality.

ACKNOWLEDGMENT

The authors would like to thank the Laboratory of Unitary Operations (109) of the Franciscan University (UFN) for the technical support for carrying out this work.

REFERENCES

Alcântara, R. R. **Synthesis, characterization, of zeolitic nanomaterial of organomodified coal ash and application as an adsorbent in the remediation of water contaminated by Rodamine B and Direct Blue 71**. 2016. Doctoral thesis. University of São Paulo.

Akhtar, M.; Iqbal, S.; Kausar, A.; Bhanger, M. I.; Shaheen, M. A. An economically viable method for the removal of selected divalent metal ions from aqueous solutions using activated rice husk. **Colloids and Surfaces: Biointerfaces**, v. 75, p. 149-155, 2010.

Böer, S. C. **Ammoniacal nitrogen adsorption of industrial effluents, from the synthesis of the Na-P1 zeolite of heavy coal ash**. 2013.

Castilla, M. C. **Eliminación de Contaminants Orgânicos de las aguas by adsorción in carbón materiales**. Department of Inorganic Chemistry, Faculty of Science, University of Granada, Spain, 2004.

Chaves, T. F.; Queiroz, Z. F.; Sousa, D. N. R.; Girão, J. H. Use of rice husk ash (RHA) obtained from thermal energy generation as Zn (II) adsorbent in aqueous solutions. **Química Nova**, v. 32, p. 1378-1383, 2009.

Della, V. P. *et al.* Recycling of agro-industrial waste: rice husk ash as an alternative source of silica. **Industrial Ceramics**, v. 10, n. 2, p. 22-25, 2000.

Birth, R. F. *et al.* **Adsorption: Theoretical aspects and environmental applications**. 1st ed. Fortaleza: University Press, 2014.

Freundlich, H. The theory of adsorption. **Zeitschriftfuer Chemie und Industrie der Kolloide**, v. 3, p. 212-220, 1909.

Gautam, R. K. *et al.* Biomass-derived biosorbents for metal ions sequestration: Adsorbent modification and activation methods and adsorbent regeneration. **Journal of Environmental Chemical Engineering**, v. 2, n. 1, p. 239-259, 2014.

Grassi, M. *et al.* Removal of emerging contaminants from water and effluents by adsorption process. In: **Removal of emerging compounds from wastewater**. Springer, Dordrecht, 2012. p. 15-37.

Gupta, V. K. *et al.* Adsorption of carmoisine A from wastewater using waste materials-Bottom ash and deoiled soya. **Journal of Colloid and Interface Science**, v. 335, p. 24-33, 2009.

Khan, R. *et al.* Microbial decolorization and degradation of synthetic dyes: a review. **Reviews in Environmental Science and Bio/Technology**, v. 12, p. 75-97, 2013.

Katheresan, V. *et al.* Efficiency of various recent wastewater dye removal methods: A review. **Journal of Environmental Chemical Engineering**, v. 6, p. 4676-4697, 2018.

Langmuir, I. The adsorption of gases on plane surfaces of glass, mica and platinum. **Journal of the American Chemical Society**, v. 40, p. 1361-1402, 1918.

Cortez, L.; Lora, E.; Gómez, E. O. **Biomassa para energia**, v. 2, p. 241-332, 2008.

Malik, P. K. Use of activated carbons prepared from sawdust and rice-husk for adsorption of acid dyes: a case study of Acid Yellow. **Dyes and Pigments**, v. 3, p. 239-249, 2003.

Machado, E. L. *et al.* Use of ozonization for the treatment of dye wastewaters containing Rhodamine B in the agate industry. **Water, Air, & Soil Pollution**, v. 223, n. 4, p. 1753-1764, 2012.

Oliveira, S. P. *et al.* Evaluation of the adsorption capacity of methylene blue dye in aqueous solutiones in natural kaolinite and interspersed with potassium acetate. **Ceramics**, v. 59, n. 350, p. 338-344, 2013.

Oliveira, F. M. *et al.* Evaluation of the adsorption process using green coconut mesocarp for removal of methylene blue dye. **Matéria (Rio de Janeiro)**, v. 23, n. 4, 2018.

Oviedo, L. R. *et al.* Antibacterial activity of nanozeolite doped with silver and titanium nanoparticles. **Journal of Sol-Gel Science and Technology**, v. 101, p. 235-243, 2022.

Rodrigues, A. C. **Effluent treatment of agate dyeing by advanced oxidative process: Fenton technique for rodamine B degradation**. 2015.

Salles, T. D. *et al.* Effective diuretic drug uptake employing magnetic carbon nanotubes derivatives: Adsorption study and in vitro geno-cytotoxic assessment. **Separation and Purification Technology**, v. 315, p. 123713, 2023.

Severo, F. F. *et al.* Chemical and physical characterization of rice husk biochar and ashes and their iron adsorption capacity. **SN Applied Sciences**, v. 2, n. 7, p. 1-9, 2020.

Vargas, G. O. Highly furosemide uptake employing magnetic graphene oxide: DFT modeling combined to experimental approach. **Journal of Molecular Liquids**, v. 379, p. 121652, 2023.

Zanella, O. **Nitrate sorption in activated carbon treated with CaCl2: Study of sorption/regeneration cycles**. 20012. 135 p. Dissertation (Master-Graduate Program in Chemical Engineering) - Department of Chemical Engineering, Federal University of Rio Grande do Sul, Porto Alegre, 2012.

Zazycki, M. A. *et al.* New biochar from pecan nutshells as an alternative adsorbent for removing reactive red 141 from aqueous solutions. **Journal of Cleaner Production**, v. 171, p. 57-65, 2018.

Zazycki, M. A. Chitin derived biochar as an alternative adsorbent to treat colored effluents containing methyl violet dye. **Advanced Powder Technology**, v. 30, p. 1494-1503, 2019.

Zazycki, M. A. Conversion of MDF wastes into a char with remarkable potential to remove Food Red 17 dye from aqueous effluents. **Chemosphere**, v. 250, p. 126248-126248, 2020.